Volume 4 | Number 3 | March 2020

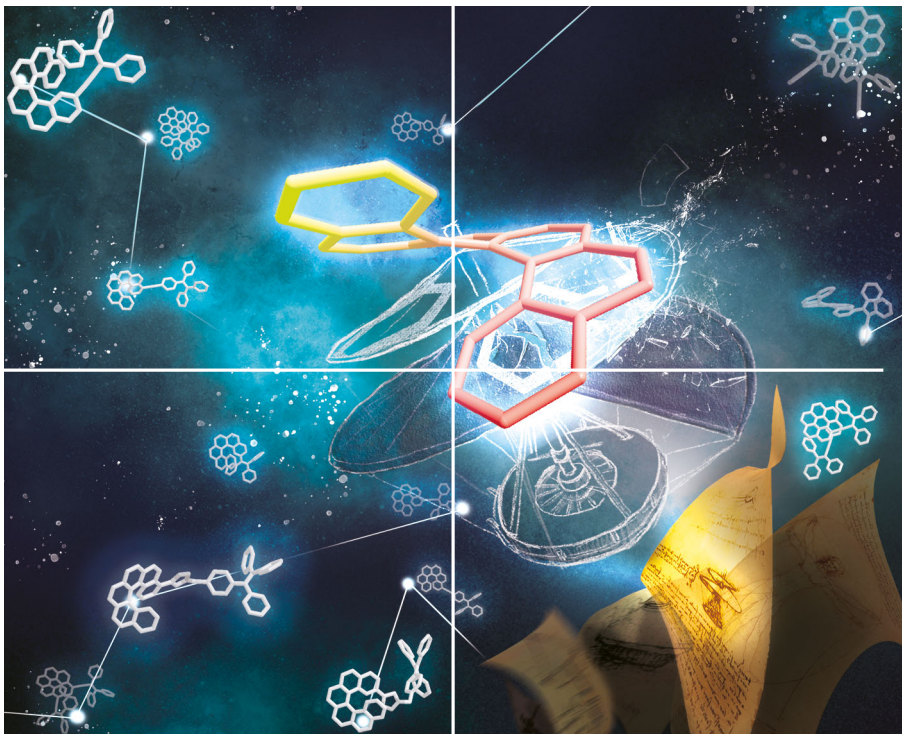

MATERIALS CHEMISTRY

FRONTIERS

CCS 中国化学会 CHINESE CHEMICAL SOCIETY

ICCAS 1956

ROYAL SOCIETY OF CHEMISTRY

rsc.li/frontiers-materials

MATERIALS CHEMISTRY FRONTIERS

RESEARCH ARTICLE

View Article Online
View Journal | View Issue

Check for updates

Cite this: *Mater. Chem. Front.*, 2020, **4**, 837

Helicene-derived aggregation-induced emission conjugates with highly tunable circularly polarized luminescence†

Chengshuo Shen,[ab] Fuwei Gan,[a] Guoli Zhang,[a] Yongle Ding,[a] Jinghao Wang,[a] Ruibin Wang,[c] Jeanne Crassous[d] and Huibin Qiu*[ab]

Received 23rd October 2019,
Accepted 20th November 2019

DOI: 10.1039/c9qm00652d

rsc.li/frontiers-materials

Published on 21 2019. Downloaded on 14/09/25 21:25:45.

Chiral organic molecules play an important role in generating circularly polarized luminescence (CPL) with high quantum yield and tunable colours. However, their CPL performance is virtually limited by the small dissymmetric factor $|g_{lum}|$ value and the aggregation-caused quenching issue in the solid state. Here, we report a series of luminescent molecules with tailored marriage of helicenes and aggregation-induced emission (AIE) luminophores. The resulting adducts are highly fluorescent in the aggregated state with colour varying from blue to green and quantum yield up to 37.0%, depending on the linkage position, conjugation and length. The efficient association of the helical conjugated skeleton of helicene and the AIE moiety also enables a relatively high $|g_{lum}|$ value ranging from 0.001 to 0.011. Notably the $|g_{lum}|$ value could be further enhanced to *ca.* 0.015 by the substitution of two AIE luminophores onto a single helicene. This work provides a practical synthetic strategy for advanced molecular CPL materials, and would also favour the fabrication of high-performance circularly polarized organic light-emitting devices.

Introduction

Circularly polarized light is a type of electromagnetic waves with its electric field vector turning along a helical trajectory, and can be distinguished as right- and left-handed lights according to its handedness.[1] In nature, species such as beetles and shrimps prevalently use circularly polarized light in signalling or covert communication.[2–4] For practical applications, circularly polarized light is also of crucial importance in quantum teleportation,[5] information encryption and storage,[6,7] chemical and biological probing,[8–11] asymmetric photosynthesis,[12,13] and electrooptical devices.[14–18] Recently, circularly polarized luminescence (CPL) materials are emerging as a key portal to generate circularly polarized light and can directly emit circularly polarized light without using a circularly polarized filter.[19] Among all CPL materials, chiral organic molecules[20–22] play an indispensable role prominently as a result of their tunable colour, strong intensity, high stability and facile processing characters compared with other materials such as chiral lanthanides[23] and chiral assembly systems.[24,25] However, the practical utilization of CPL-active organic molecules is substantially limited by the low dissymmetric factor $|g_{lum}|$ ($g_{lum} = 2(I_L - I_R)/(I_L + I_R)$, where I_L and I_R are the intensities of left- and right-handed circularly polarized emissions, respectively) and the potential aggregation-caused luminescence quenching in the solid state.

Aggregation-induced emission (AIE) provides an effective way to overcome the aggregation-caused luminescence quenching issue[26,27] and appears to be useful for the construction of new CPL materials. However, most of the CPL active AIE materials were achieved *via* supramolecular, polymer or liquid crystal pathways,[25] which substantially limits the further applications due to the intensive dependence on ordered supramolecular structures and the obscure structure–function relationship. To date, only a few CPL active AIE small molecules have been prepared, mainly by tethering chiral binaphthyl elements onto AIE luminophores.[28,29] Nevertheless, the $|g_{lum}|$ value of these molecular materials was found to be less than 5×10^{-3}, probably as a consequence of the insufficient association between the chiral elements and the AIE luminophores.

Helicenes are constituted of *ortho*-fused spirally arranged aromatic rings, and exhibit prominent chiroptical properties

[a] *School of Chemistry and Chemical Engineering, State Key Laboratory of Metal Matrix Composites, Shanghai Jiao Tong University, Shanghai 200240, China. E-mail: hbqiu@sjtu.edu.cn*
[b] *State Key Laboratory for Modification of Chemical Fibers and Polymer Materials, College of Materials Science and Engineering, Donghua University, Shanghai 201620, China*
[c] *Instrumental Analysis Center, Shanghai Jiao Tong University, Shanghai 200040, China*
[d] *Univ Rennes, Institut des Sciences Chimiques de Rennes, UMR CNRS 6226, Campus de Beaulieu, Rennes 35042, France*

† Electronic supplementary information (ESI) available: Experimental details and structural characterization including NMR, MS and single crystal structures; UV, ECD, PL spectra; theoretical calculation details. CCDC 1960871–1960879. For ESI and crystallographic data in CIF or other electronic format see DOI: 10.1039/c9qm00652d

Published on 21 2019. Downloaded on 14/09/25 21:25:45.

because of the large rotational strength from the inherent electron transitions along the helical π-conjugated skeleton.[30,31] Compared with other chiral organic molecules, helicene derivatives are of great importance for CPL materials due to their relatively large CPL signals.[21,32–37] Here, we develop a practical pathway to prepare highly luminescent AIE materials with tunable emission colour and high $|g_{lum}|$ value by tethering or fusing helicene units as a chiral auxiliary onto AIE-active tetraphenylethene (TPE) units. Through flexible marriage of AIE luminophores with ready-made helicenes by click chemistry or metal-catalysed coupling reactions, a series of AIE–helicene adducts have been synthesized, and they exhibit blue to green emission colours (λ_{em} = 450–520 nm) in the aggregated state with a quantum yield (Φ) of 3.8–37.0% and $|g_{lum}|$ value up to 0.015. This work provides new opportunities for the design and synthesis of advanced CPL materials, which would be useful for the preparation of high-performance circularly polarized light-emitting devices.

Results and discussion

Non-conjugated AIE–helicene adducts

TPE is a typical AIE luminophore and exhibits strong luminescence towards aggregation (Φ = 49.2% in film).[38,39] It was anticipated that by close linking, the chirality of helicene can be transferred to the TPE luminophore and thus induce CPL (Fig. 1a). To this end, we first synthesized two adducts, namely **2-TBTH** and **4-TBTH**, by tethering TPE onto 2- and 4-ethynyl[6]-helicenes, respectively, through click chemistry (copper-catalysed azide–alkyne cycloaddition reaction) (Fig. 1b, see the ESI† for synthetic details).

As shown in Fig. 1c, both **2-TBTH** and **4-TBTH** showed positive Cotton effects around 335 and 330 nm and negative Cotton effects around 270 and 252 nm for the *P*-enantiomers (mirror image for the *M*-enantiomers), respectively, indicating a characteristic nature of [6]helicene. When investigating the luminescence property (Fig. 1d), to our surprise, these two molecules failed to exhibit typical AIE properties. Along with an increase of the water fraction from 0% to 95%, the luminescence showed no obvious enhancement (see Fig. S44 and S45, ESI† for luminescence spectra with different water fractions) and the quantum yields in the aggregated state were only 3.8% and 5.6%, much smaller than TPE itself. This was probably because the helicene moiety emits both in solution and in the aggregated state, and the relatively loose aggregation structures might also impair the AIE feature of the TPE domain. Regarding their CPL performance, **2-TBTH** was found to be CPL active and showed relatively high g_{lum} values of +0.012 and −0.010 for the *P*- and *M*-enantiomers (at *ca.* 450 nm, maximum emission wavelength, $\lambda_{em,max}$), respectively. In contrast, **4-TBTH** was found to be CPL inactive.

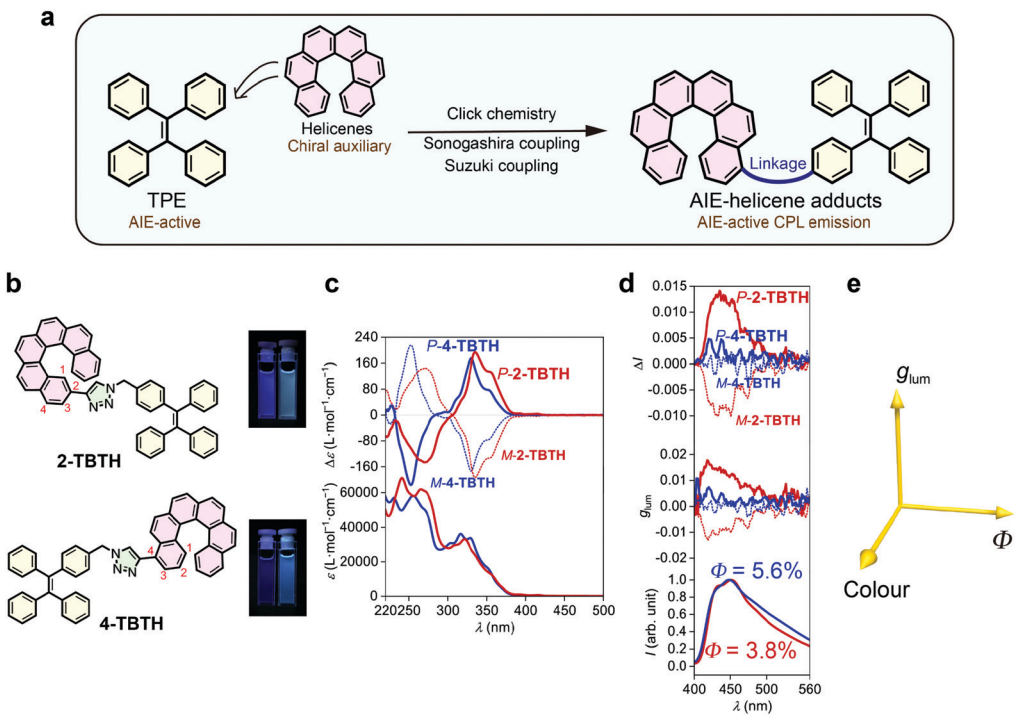

Fig. 1 Design of AIE–helicene adducts and CPL performance of non-conjugated AIE–helicene adducts. (a) Illustrative representation for the synthetic strategy of AIE–helicene adducts *via* tunable linking of helicenes (as chiral auxiliary) and AIE-active TPE units through click chemistry, Sonogashira coupling and Suzuki coupling reactions. (b) Molecular structures of **2-TBTH** and **4-TBTH**, and the corresponding photographs showing their luminescence behaviour in THF (left) and a mixture of THF and H_2O (1 : 19, v/v) (right) with a concentration of 2.0 × 10^{-5} mol L^{-1} under 365 nm UV light irradiation. (c) UV-vis and ECD spectra of **2-TBTH** and **4-TBTH** in THF with a concentration of 2.0 × 10^{-5} mol L^{-1} at 298 K. (d) Luminescence, CPL and g_{lum} spectra of **2-TBTH** and **4-TBTH** in a mixture of THF and H_2O (1 : 19, v/v) with a concentration of 2.0 × 10^{-5} mol L^{-1} at 298 K with excitation at 365 nm. (e) Three key factors (g_{lum}, quantum yields Φ, and colour) for the evaluation of CPL materials.

 This journal is © The Royal Society of Chemistry and the Chinese Chemical Society 2020

Published on 21 2019. Downloaded on 14/09/25 21:25:45.

Fully conjugated AIE–helicene adducts

Although the g_{lum} of **2-TBTH** appears to be prominent (presumably majorly derived from the helicene-triazole moiety), its quantum yield is extremely low and the emission colour is limited in the blue region. In principle, an ideal CPL material system should be characterized by a high $|g_{lum}|$ value, a high quantum yield and a large diversity in emitting colour (Fig. 1e). To this end, we further prepared **2-TPEH** and **4-TPEH** (Fig. 2a left, see the ESI† for synthetic details) by linking helicene and TPE through a conjugated alkynyl bridge.[40,41]

In the absorption spectra (Fig. 2b left), both **2-TPEH** and **4-TPEH** showed a bathochromic shift for the major bands with the absorption extending to >400 nm, clearly reflecting a strong π-conjugation between helicene and TPE through the alkynyl bridge. The ECD curves of *P*- and *M*-**2-TPEH** revealed a series of Cotton effects which were significantly shifted into the longer wavelength region compared to that of the pristine [6]helicene (see Fig. S56 and S57, ESI† for comparison),[42] echoing the extension of π-conjugation observed in the absorption spectra.[43] In a tremendous contrast, *P*- and *M*-**4-TPEH** showed analogous Cotton effects like the pristine [6]helicene in the relatively shorter wavelength region even though the absorption curves were apparently bathochromically shifted.

Both **2-TPEH** and **4-TPEH** showed typical AIE feature where no obvious emission was observed in the THF solution, but upon aggregation with the water fraction increased to 95% (see Fig. S46 and S47, ESI† for luminescence spectra with different water fractions), strong green luminescence centred at *ca.* 500 nm was detected with high quantum yields of 33.9% and 37.0%, respectively (Fig. 2c left). Importantly, **2-TPEH** was CPL active with $|g_{lum}|$ = *ca.* 0.001 at 500 nm, while **4-TPEH** was inactive.

To decrease the distance between helicene and the AIE luminophore and hence possibly promote the chirality transfer from helicene to TPE, next, we prepare **TEH** and **TH** by removing the connective benzene ring of TPE and further the CC triple

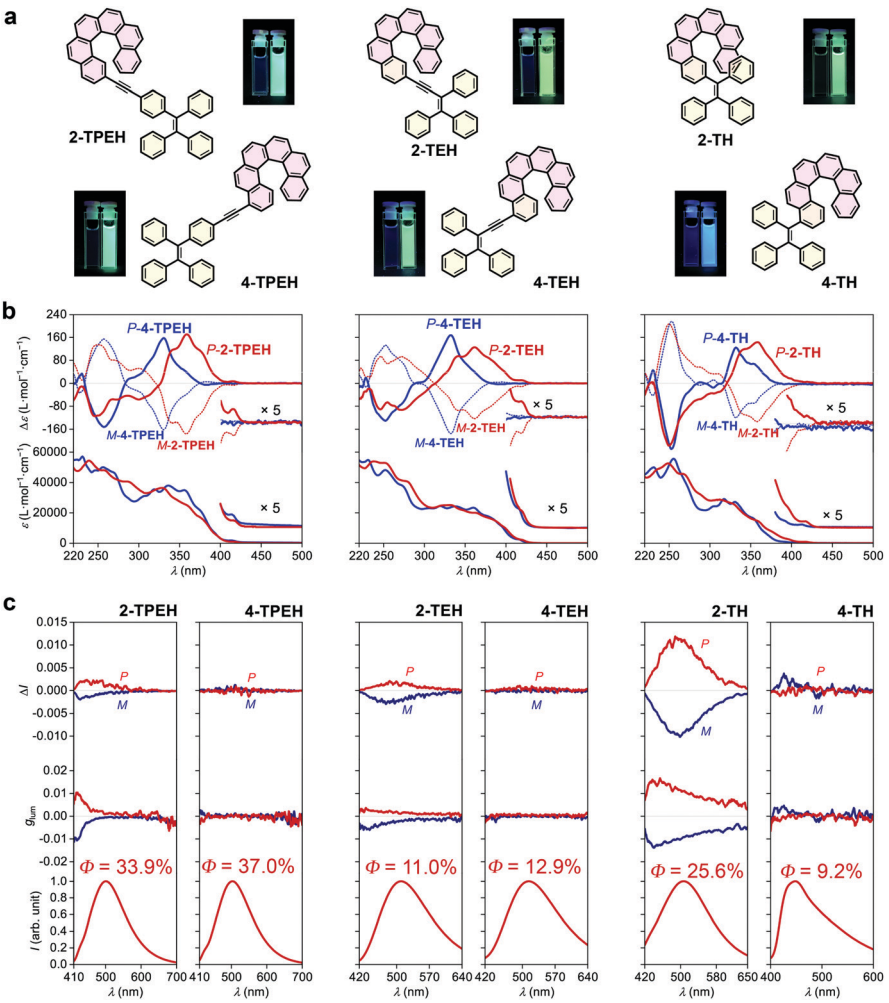

Fig. 2 Fully conjugated AIE–helicene adducts. (a) Molecular structures of **TPEH**, **TEH** and **TH** with different substitution positions (2 and 4) and the corresponding photographs showing their luminescence behaviour in THF (left) and a mixture of THF and H_2O (1 : 19, v/v) (right) with a concentration of 2.0×10^{-5} mol L^{-1} under 365 nm UV light irradiation. (b) UV-vis and ECD spectra of **TPEH**, **TEH** and **TH** in THF with a concentration of 2.0×10^{-5} mol L^{-1} at 298 K. (c) Luminescence, CPL and g_{lum} spectra of **TPEH**, **TEH** and **TH** in a mixture of THF and H_2O (1 : 19, v/v) with a concentration of 2.0×10^{-5} mol L^{-1} at 298 K with excitation at 365 nm.

Published on 21 2019. Downloaded on 14/09/25 21:25:45.

bond (Fig. 2a middle and right, see the ESI† for synthetic details). **2-TEH**, **4-TEH** and **2-TH** showed stronger absorption in the visible region (>400 nm), indicating a well-conjugated structure similar to **TPEH**. Nevertheless, **4-TH** showed no obvious absorption >380 nm, probably because the huge steric hindrance weakened the conjugation. As shown in Fig. 2b middle and right, similar to **2-TPEH**, **2-TEH** and **2-TH** showed relatively bathochromically shifted Cotton effects compared with the pristine carbo[6]helicene, while **4-TEH** and **4-TH** exhibit analogous CD curves like **4-TPEH** (see Fig. S56 and S57, ESI† for comparison).

It was found that **2-TEH**, **4-TEH** and **2-TH** were typically AIE active and showed green luminescence ($\lambda_{em,max}$ = 510, 515 and 506 respectively) in the aggregated state (Fig. 2c middle and right, Fig. S48, S49 and S52, ESI†). For **2-TEH** and **4-TEH**, although the AIE luminophore only has three phenyl rings, the adducts retained the AIE feature and displayed moderated quantum yields of 11.0% and 12.9%, respectively (Fig. 2c middle). For **2-TH**, the aggregates revealed a significantly higher quantum yield (up to 25.6%) (Fig. 2c right), indicating a more confined and rigid molecular structure in the aggregated state, probably due to the closer approximation of the helicene and AIE moieties. In contrast, **4-TH** was slightly blue fluorescent in the solution and revealed aggregation-induced emission enhancement behaviour upon aggregation (Fig. S53, ESI†), where a blue emission colour and a relatively low quantum yield of 9.2% were detected (Fig. 2c right). Both **2-TEH** and **2-TH** are CPL active with a $|g_{lum}|$ value of *ca.* 0.002 (at $\lambda_{em,max}$ = 506 nm) and 0.011 (at $\lambda_{em,max}$ = 515 nm), respectively. Apparently, the CPL performance was improved by shortening the distance between helicene and the AIE luminophore. Besides, for **2-TH**, the spatial regulation of the phenyl rings of the AIE moiety (into a certain chiral arrangement) by helicene through steric hindrance would be another key factor for a higher $|g_{lum}|$ value. Interestingly, the 4-substituted adducts (**4-TEH** and **4-TH**) again kept CPL silent in the whole emission region, indicating a strong effect of substitution position on the CPL performance.

Bis-substituted AIE–helicene adducts

The introduction of two luminophores at both ends of helicene has been demonstrated to be an efficient pathway to tune the chiroptical properties, mainly through exciton coupling of the pedant luminophores.[41] We then synthesized **2,15-BTEH**, **4,13-BTEH**, **2,15-BTH** and **4,13-BTH** by tethering two AIE luminophores onto a single helicene (Fig. 3a, see the ESI† for synthetic details).

The absorption spectra of all four bis-substituted AIE–helicene adducts displayed a slightly bathochromic shift compared with their mono-substituted homologues and showed stronger ε values (*e.g.*, $>7 \times 10^4$ L mol^{-1} cm^{-1} at *ca.* 250 nm)

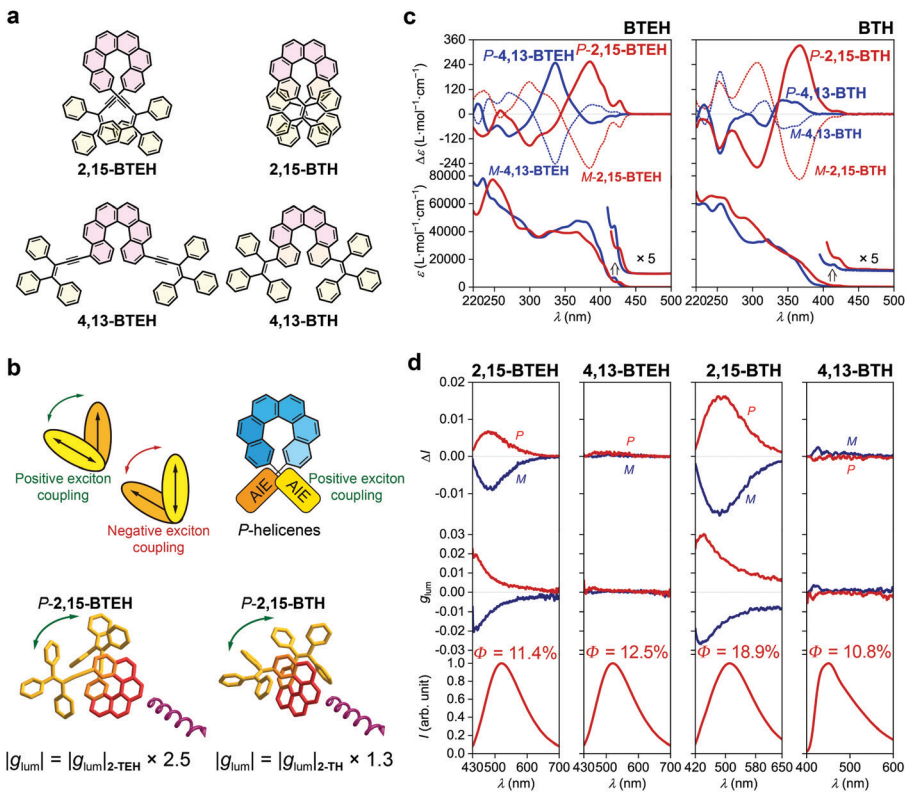

Fig. 3 Bis-substituted AIE–helicene adducts. (a) Molecular structures of **2,15-BTEH**, **4,13-BTEH**, **2,15-BTH** and **4,13-BTH**. (b) Illustrative representation of exciton couplings and crystal structures of *P*-**2,15-BTEH** and *P*-**2,15-BTH** with a positive exciton coupling and consequently, an enhanced $|g_{lum}|$ value compared to the mono-substituted **2-TEH** and **2-TH** analogues, respectively. (c) UV-vis and ECD spectra of **BTEH** and **BTH** in THF with a concentration of 2.0×10^{-5} mol L^{-1} at 298 K. (d) Luminescence, CPL and g_{lum} spectra of **BTEH** and **BTH** in a mixture of THF and H_2O (1 : 19, v/v) with a concentration of 2.0×10^{-5} mol L^{-1} at 298 K with excitation at 365 nm.

 This journal is © The Royal Society of Chemistry and the Chinese Chemical Society 2020

Published on 21 2019. Downloaded on 14/09/25 21:25:45.

probably due to the additional luminophores (Fig. 3c). However, the absorption bands were limited in the range of <440 nm, without strong extension to the longer wavelength compared with their mono-substituted analogues, indicating a weak conjugation between the two luminophores through the helicene backbone. In the ECD spectra, both *P*-**2,15-BTEH** and *P*-**4,13-BTEH** showed a significantly increased Cotton effect at 385 nm ($\Delta\varepsilon$ = +253 L mol^{-1} cm^{-1}) and 336 nm ($\Delta\varepsilon$ = +247 L mol^{-1} cm^{-1}), respectively. Interestingly, for *P*-**2,15-BTH**, the intensity ($\Delta\varepsilon$ = +332 L mol^{-1} cm^{-1}) of the Cotton effect at 366 nm also doubled compared to the mono-substituted **2-TH**. However, for *P*-**4,13-BTH**, the intensity of the Cotton effect at 340 nm was diminished to +68 L mol^{-1} cm^{-1}, just half of that shown by **4-TH**.

The emission of these bis-substituted AIE–helicene adducts inherited the feature of their mono-substituted analogues. For example, **2,15-BTEH**, **4,13-BTEH** and **2,15-BTH** displayed typical AIE features with a green emission colour with $\lambda_{em,max}$ = *ca.* 510 to 520 nm, and **4,13-BTH** showed a blue emission with a relatively low quantum yield (10.8%). Both **2,15-BTEH** and **2,15-BTH** were CPL active and showed a significantly increased $|g_{lum}|$ value of *ca.* 0.005 (at $\lambda_{em,max}$ = 520 nm, *ca.* 2.5 folders of **2-TEH**) and 0.015 (at $\lambda_{em,max}$ = 510 nm, *ca.* 1.3 folders of **2-TH**), respectively (Fig. 3b and d). However, for **4,13-BTEH** and **4,13-BTH**, no obvious CPL signal was detected.

Generally, g_{lum}, emitting colour and quantum yield can be recognized as the three key factors for the evaluation of CPL materials (Fig. 1e). Amongst them, emitting colour and quantum yield determine the luminescence property and are universal for all luminescent materials. However, g_{lum} is specifically associated with chiral luminescent materials, which reflects the ability of emitting circularly polarized light. In this work, we were able to modulate these three factors by tuning of the linkage between helicene and the AIE luminophores (Fig. 4).

The linkage position shows dominating influence on the CPL signals (Fig. 4a). In this work, all the 2- (or 2,15-) substituted

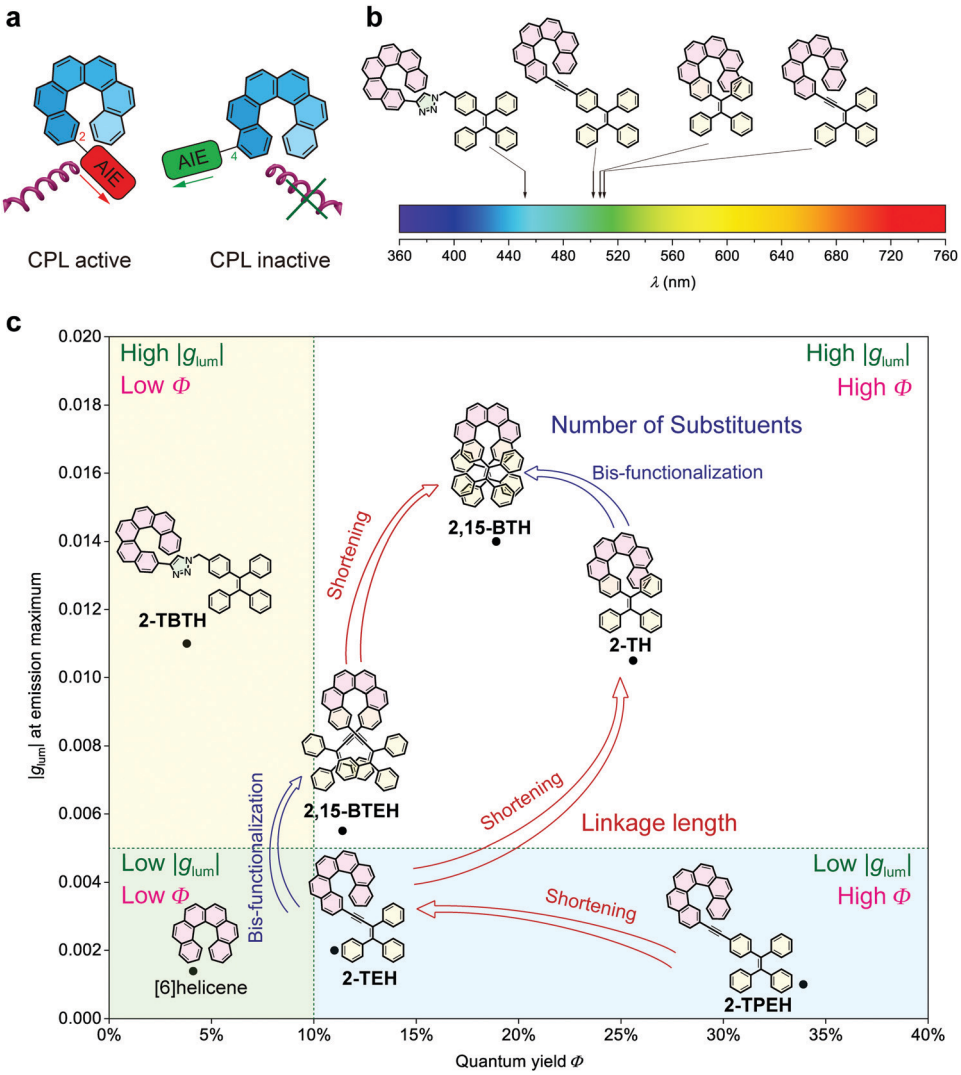

Fig. 4 Rules for CPL performance of AIE–helicene adducts. (a) Effect of linkage position on CPL capability. (b and c) Effect of linkage conjugation and length, and number of substituents on (b) emission colour and (c) $|g_{lum}|$ and quantum yield Φ.

Published on 21 2019. Downloaded on 14/09/25 21:25:45.

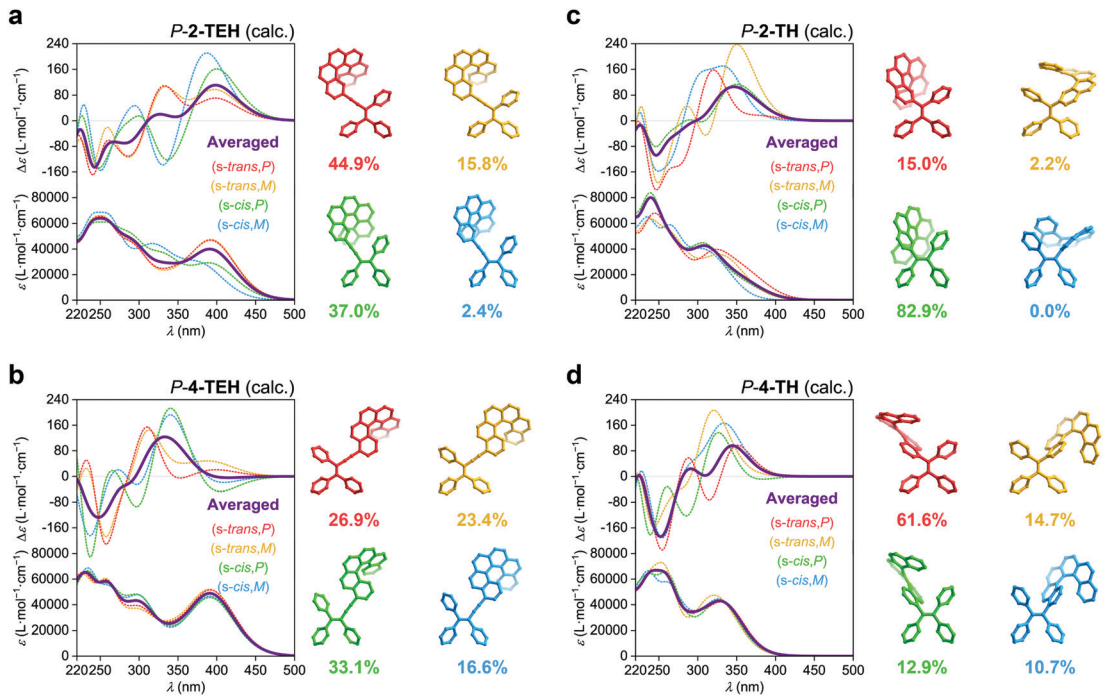

Fig. 5 Theoretical calculation results of **TEH** and **TH**. DFT-optimized structures of the four most reasonable rotamers with a relative occupancy estimated from Boltzmann distribution at 298.15 K for (a) *P*-**2-TEH**, (b) *P*-**4-TEH**, (c) *P*-**2-TH** and (d) *P*-**4-TH**, and their calculated absorption and ECD spectra (dash lines) and the averaged absorption and ECD spectra (purple solid lines). DFT and TD-DFT calculations were performed at the B3LYP/6-311G(d,p) level with SMD continuum solvent model for THF, and the spectra were simulated following a Gaussian function centred at vertical excitation energies with a half-width at half height of 0.25 eV and were shifted by +0.2 eV for better matching. The averaged spectra were weighted by the relative occupancy.

AIE–helicene adducts appear to be CPL active while all the 4- (or 4,13-) substituted analogues are CPL inactive. This probably can be interpreted by the cancellation of contributions from various rotational conformers (rotamers) (Fig. 5). For **2-TEH** and **2-TH**, we found that the four most reasonable rotamers all provide positive ECD signals in the region >380 nm for the *P* enantiomers. In contrast, the ECD signal of **4-TEH** or **4-TH** in the larger wavelength region varies with different conformations, and the averaged ECD spectra show a serious cancellation. The CPL performance (emission corresponding to the S_1 to S_0 transition) of these molecules is strongly associated with the ECD in the lower energy band (absorption corresponding to the S_0 to S_1 transition).[21] Consequently, the 2-substituted adducts are CPL active, while the 4-substituted analogues appear to be CPL silent. It should be noted that the linkage position also shows an obvious influence on the emitting colour and quantum yield for the **TH** and **BTH** derivatives.

On the other hand, the linkage conjugation mainly tunes the emitting colour. For **TBTH**, due to the break of conjugation, the emitting colour is limited in the blue region. In contrast, the full conjugation of the helicene and AIE luminophore moieties in **TPEH**, **TEH** and **TH** reduces the energy gap of the electronic transitions, causing the emission bands both to shift to the longer wavelength region (Fig. 4b). Besides, the conjugated linkages generally guarantee the AIE performance and a relatively high quantum yield in the aggregated state.

Compared to other variations, the linkage length predominantly modulates g_{lum}. With a decrease in the linkage length, the $|g_{lum}|$ value increases from 0.001 for **2-TPEH** to 0.002 for **2-TEH** and to 0.011 for **2-TH** (Fig. 4c). It is postulated that the shorter linkage facilitates the chirality transfer from helicene to the whole molecular skeleton and also reinforces the chirality regulation of the conformation of the AIE luminophore by the helicene moiety *via* steric hindrance. This is indicated by the DFT calculations on the occupancy of various rotamers for **2-TEH** and **2-TH** (compare Fig. 5a and c). Moreover, the shorter linkage also promotes the orbital association of helicene and the AIE luminophore, which would be helpful for a higher $|g_{lum}|$ value. Notably, the number of linkages is another important factor for g_{lum} modulation.

Conclusions

In summary, we have demonstrated a practical pathway to prepare CPL-active AIE materials by flexible tethering of helicene and AIE luminophores. The resulting adducts showed tunable emission colours from blue to green, high luminescence intensity (quantum yield up to 37%), and large $|g_{lum}|$ values up to 0.015 in the aggregated state. These AIE–helicene adducts are expected to be employed for further applications in, for example, organic light-emitting diodes with circularly polarized light emission and anti-fake polarized inks. Besides, the synthetic methods and structure-performance rules developed in this work would also be useful for the construction of advanced CPL materials.

 This journal is © The Royal Society of Chemistry and the Chinese Chemical Society 2020

Conflicts of interest

There are no conflicts to declare.

Acknowledgements

This work was supported by the National Natural Science Foundation of China (21704063), the Science and Technology Commission of Shanghai Municipality (17YF1412100, 17JC1400700 and 18JC1415500), and the Shanghai Education Development Foundation and the Shanghai Municipal Education Commission (16SG54). The authors thank Prof. Youxuan Zheng from Nanjing University for help with CPL measurements.

Published on 21 2019. Downloaded on 14/09/25 21:25:45.

Notes and references

1 G. H. Wagnière in *Comprehensive Chiroptical Spectroscopy*, ed. N. Berova, P. L. Polavarapu, K. Nakanishi and R. W. Woody, John Wiley & Sons, Inc, Hoboken, 2012, vol. 2, pp. 3–34.
2 V. Sharma, M. Crne, J. O. Park and M. Srinivasarao, Structural Origin of circularly polarized iridescence in jeweled beetles, *Science*, 2009, **325**, 449.
3 T.-H. Chiou, S. Kleinlogel, T. Cronin, R. Caldwell, B. Loeffler, A. Siddiqi, A. Goldizen and J. Marshall, Circular polarization vision in a stomatopod crustacean, *Curr. Biol.*, 2008, **18**, 429.
4 Y. L. Gagnon, R. M. Templin, M. J. How and N. J. Marshall, Circularly polarized light as a communication signal in mantis shrimps, *Curr. Biol.*, 2015, **25**, 3074.
5 J. F. Sherson, H. Krauter, R. K. Olsson, B. Julsgaard, K. Hammerer, I. Cirac and E. S. Polzik, Quantum teleportation between light and matter, *Nature*, 2006, **443**, 557.
6 C. Wang, H. Fei, Y. Qiu, Y. Yang and Z. Wei, Photoinduced birefringence and reversible optical storage in liquid-crystalline azobenzene side-chain polymers, *Appl. Phys. Lett.*, 1998, **74**, 19.
7 H. Zheng, W. Li, W. Li, X. Wang, Z. Tang, S. X.-A. Zhang and Y. Xu, Uncovering the circular polarization potential of chiral photonic cellulose films for photonic applications, *Adv. Mater.*, 2018, **30**, 1705948.
8 M. Seitz, E. G. Moore, A. J. Ingram, G. Muller and K. N. Raymond, Enantiopure, octadentate ligands as sensitizers for europium and terbium circularly polarized luminescence in aqueous solution, *J. Am. Chem. Soc.*, 2007, **129**, 15468.
9 J. Yuasa, T. Ohno, H. Tsumatori, R. Shiba, H. Kamikubo, M. Kataoka, Y. Hasegawa and T. Kawai, Fingerprint signatures of lanthanide circularly polarized luminescence from proteins covalently labeled with a β-diketonate europium(III) chelate, *Chem. Commun.*, 2013, **49**, 4604.
10 F. Song, G. Wei, X. Jiang, F. Li, C. Zhu and Y. Cheng, Chiral sensing for induced circularly polarized luminescence using an Eu(III)-containing polymer and D- or L-proline, *Chem. Commun.*, 2013, **49**, 5772.
11 S. Shuvaev, E. A. Suturina, K. Mason and D. Parker, Chiral probes for α_1-AGP reporting by species-specific induced circularly polarised luminescence, *Chem. Sci.*, 2018, **9**, 2996.
12 I. Sato, R. Sugie, Y. Matsueda, Y. Furumura and K. Soai, Asymmetric synthesis utilizing circularly polarized light mediated by the photoequilibrium of chiral olefins in conjunction with asymmetric autocatalysis, *Angew. Chem., Int. Ed.*, 2004, **43**, 4490.
13 R. D. Richardson, M. G. J. Baud, C. E. Weston, H. S. Rzepa, M. K. Kuimova and M. J. Fuchter, Dual wavelength asymmetric photochemical synthesis with circularly polarized light, *Chem. Sci.*, 2015, **6**, 3853.
14 J. Han, S. Guo, H. Lu, S. Liu, Q. Zhao and W. Huang, Recent progress on circularly polarized luminescent materials for organic optoelectronic devices, *Adv. Opt. Mater.*, 2018, **6**, 1800538.
15 Y. Yang, R. C. da Costa, M. J. Fuchter and A. J. Campbell, Circularly polarized light detection by a chiral organic semiconductor transistor, *Nat. Photonics*, 2013, **7**, 634.
16 Y. Yang, R. C. da Costa, D.-M. Smilgies, A. J. Campbell and M. J. Fuchter, Induction of circularly polarized electroluminescence from an achiral light-emitting polymer *via* a chiral small-molecule dopant, *Adv. Mater.*, 2013, **25**, 2624.
17 J. R. Brandt, X. Wang, Y. Yang, A. J. Campbell and M. J. Fuchter, Circularly polarized phosphorescent electroluminescence with a high dissymmetry factor from PHOLEDs based on a platinahelicene, *J. Am. Chem. Soc.*, 2016, **138**, 9743.
18 J. Han, S. Guo, J. Wang, L. Wei, Y. Zhuang, S. Liu, Q. Zhao, X. Zhang and W. Huang, Circularly polarized phosphorescent electroluminescence from chiral cationic iridium(III) isocyanide complexes, *Adv. Opt. Mater.*, 2017, **5**, 1700359.
19 J. P. Riehl and F. S. Richardson, Circularly polarized luminescence spectroscopy, *Chem. Rev.*, 1986, **86**, 1.
20 E. M. Sánchez-Carnerero, A. R. Agarrabeitia, F. Moreno, B. L. Maroto, G. Muller, M. J. Ortiz and S. de la Moya, Circularly polarized luminescence from simple organic molecules, *Chem. – Eur. J.*, 2015, **21**, 13488.
21 H. Tanaka, Y. Inoue and T. Mori, Circularly polarized luminescence and circular dichroisms in small organic molecules: correlation between excitation and emission dissymmetry factors, *ChemPhotoChem*, 2018, **2**, 386.
22 N. Chen and B. Yan, Recent Theoretical and experimental progress in circularly polarized luminescence of small organic molecules, *Molecules*, 2018, **23**, 3376.
23 F. Zinna and L. Di Bari, Lanthanide circularly polarized luminescence: bases and applications, *Chirality*, 2015, **27**, 1.
24 J. Kumar, T. Makashima and T. Kawai, Circularly polarized luminescence in chiral molecules and supramolecular assemblies, *J. Phys. Chem. Lett.*, 2015, **6**, 3450.
25 J. Roose, B. Z. Tang and K. S. Wong, Circularly-polarized luminescence (CPL) from chiral AIE molecules and macrostructures, *Small*, 2016, **12**, 6495.
26 Y. Hong, J. W. Y. Lam and B. Z. Tang, Aggregation-induced emission, *Chem. Soc. Rev.*, 2011, **40**, 5361.
27 J. Mei, N. L. C. Leung, R. T. K. Kwok, J. W. Y. Lam and B. Z. Tang, Aggregation-induced emission: together we shine, united we soar!, *Chem. Rev.*, 2015, **115**, 11718.

Published on 21 2019. Downloaded on 14/09/25 21:25:45.

28 S. Zhang, Y. Wang, F. Meng, C. Dai, Y. Cheng and C. Zhu, Circularly polarized luminescence of AIE-active chiral O-BODIPYs induced *via* intramolecular energy transfer, *Chem. Commun.*, 2015, **51**, 9014.
29 Y. Sheng, D. Shen, W. Zhang, H. Zhang, C. Zhu and Y. Cheng, Reversal circularly polarized luminescence of AIE-active chiral binaphthyl molecules from solution to aggregation, *Chem. – Eur. J.*, 2015, **21**, 13196.
30 Y. Shen and C.-F. Chen, Helicene: synthesis and application, *Chem. Rev.*, 2012, **112**, 1463.
31 M. Gingras, One hundred years of helicene chemistry. Part 1: non-stereoselective syntheses of carbohelicenes, *Chem. Soc. Rev.*, 2013, **42**, 968.
32 K. Nakamura, S. Furumi, M. Takeuchi, T. Shibuya and K. Tanaka, Enantioselective synthesis and enhanced circularly polarized luminescence of S-shaped double azahelicenes, *J. Am. Chem. Soc.*, 2014, **136**, 5555.
33 K. Murayama, Y. Oike, S. Furumi, M. Takeuchi, K. Noguchi and K. Tanaka, Enantioselective synthesis, crystal structure, and photophysical properties of a 1,1′-bitriphenylene-based sila[7]helicene, *Eur. J. Org. Chem.*, 2015, 1409.
34 T. Kaseyama, S. Furumi, X. Zhang, K. Tanaka and M. Takeuchi, Hierarchical assembly of a phthalhydrazide-functionalized helicene, *Angew. Chem., Int. Ed.*, 2011, **50**, 3684.
35 H. Oyama, M. Akiyama, K. Nakano, M. Naito, K. Nobusawa and K. Nozaki, Synthesis and properties of [7]helicene-like compounds fused with a fluorene unit, *Org. Lett.*, 2016, **18**, 3657.
36 C. Shen, E. Anger, M. Srebro, N. Vanthuyne, K. K. Deol, T. D. Jefferson, G. Muller, J. A. G. Williams, L. Toupet, C. Roussel, J. Autschbach, R. Réau and J. Crassous, Straightforward access to mono- and bis-cycloplatinated helicenes displaying circularly polarized phosphorescence by using crystallization resolution methods, *Chem. Sci.*, 2014, **5**, 1915.
37 C. M. Cruz, S. Castro-Fernández, E. Maçôas, J. M. Cuerva and A. G. Campaña, Undecabenzo[7]superhelicene: a helical nanographene ribbon as a circularly polarized luminescence emitter, *Angew. Chem., Int. Ed.*, 2018, **57**, 14782.
38 N. L. C. Leung, N. Xie, W. Yuan, Y. Liu, Q. Wu, Q. Peng, Q. Miao, J. W. Y. Lam and B. Z. Tang, Restriction of intramolecular motions: the general mechanism behind aggregation-induced emission, *Chem. – Eur. J.*, 2014, **20**, 15349.
39 Z. Zhao, S. Chen, J. W. Y. Lam, C. K. W. Jim, C. Y. K. Chan, Z. Wang, P. Lu, C. Deng, H. S. Kwok, Y. Ma and B. Z. Tang, Steric hindrance, electronic communication, and energy transfer in the photo- and electroluminescence processes of aggregation-induced emission luminogens, *J. Phys. Chem. C*, 2010, **114**, 7963.
40 C. Schaack, L. Arrico, E. Sidler, M. Górecki, L. Di Bari and F. Diederich, Helicene monomers and dimers: chiral chromophores featuring strong circularly polarized luminescence, *Chem. – Eur. J.*, 2019, **25**, 8003.
41 K. Dhbaibi, L. Favereau, M. Srebro-Hooper, M. Jean, N. Vanthuyne, F. Zinna, B. Jamoussi, L. Di Bari, J. Autschbach and J. Crassous, Exciton coupling in diketo-pyrrolopyrrole–helicene derivatives leads to red and near-infrared circularly polarized luminescence, *Chem. Sci.*, 2018, **9**, 735.
42 Y. Nakai, T. Mori and Y. Inoue, Theoretical and experimental studies on circular dichroism of carbo[*n*]helicenes, *J. Phys. Chem. A*, 2012, **116**, 7372.
43 M. E. S. Moussa, M. Srebro, E. Anger, N. Vanthuyne, C. Roussel, C. Lescop, J. Autschbach and J. Crassous, Chiroptical properties of carbo[6]helicene derivatives bearing extended π–conjugated cyano substituents, *Chirality*, 2013, **25**, 455.

 This journal is © The Royal Society of Chemistry and the Chinese Chemical Society 2020